

E-ELT turbulence profiling with stereo-SCIDAR at Paranal

James Osborn^a, Richard Wilson^a, Tim Butterley^a, Tim Morris^a, Marc Dubbeldam^a, Frédéric Dérié^b, and Marc Sarazin^b

^aCentre for advanced instrumentation, Durham University, UK

^bEuropean Southern Observatory, Karl-Schwarzschild-Str.2, 85748 Garching bei Muenchen, Germany

ABSTRACT

Vertical profiles of the atmospheric optical turbulence strength and velocity is of critical importance for simulating, designing, and operating the next generation of instruments for the European Extremely Large Telescope. Many of these instruments are already well into the design phase meaning these profiles are required immediately to ensure they are optimised for the unique conditions likely to be observed.

Stereo-SCIDAR is a generalised SCIDAR instrument which is used to characterise the profile of the atmospheric optical turbulence strength and wind velocity using triangulation between two optical binary stars. Stereo-SCIDAR has demonstrated the capability to resolve turbulent layers with the required vertical resolution to support wide-field ELT instrument designs. These high resolution atmospheric parameters are critical for design studies and statistical evaluation of on-sky performance under real conditions. Here we report on the new Stereo-SCIDAR instrument installed on one of the Auxillary Telescope ports of the Very Large Telescope array at Cerro Paranal. Paranal is located approximately 20 km from Cerro Armazones, the site of the E-ELT. Although the surface layer of the turbulence will be different for the two sites due to local geography, the high-altitude resolution profiles of the free atmosphere from this instrument will be the most accurate available for the E-ELT site.

In addition, these unbiased and independent profiles are also used to further characterise the site of the VLT. This enables instrument performance calibration, optimisation and data analysis of, for example, the ESO Adaptive Optics facility and the Next Generation Transit Survey. It will also be used to validate atmospheric models for turbulence forecasting. We show early results from the commissioning and address future implications of the results.

Keywords: Atmospheric instrumentation, Adaptive Optics, atmospheric turbulence

1. INTRODUCTION

Adaptive Optics (AO) can be used to correct for the detrimental effects of the atmosphere by reducing the aberration in the phase of the wavefront. AO systems are becoming more sophisticated, moving towards wide-field or high-spatial resolution applications.

It is important to be able to accurately model the performance of these systems in the design phase of future instruments in order to ensure that the instrument meets specifications. In addition, during and after commissioning it is important to be able to monitor the instrument in order to validate and optimise the performance.¹ This is enabled by high-sensitivity and high-altitude resolution vertical profiles of the optical turbulence in the Earth's atmosphere.

The large number of subapertures across the AO system pupil means that the next generation of 30 to 40 m class Extremely Large Telescopes (ELTs) will be significantly more sensitive to variations in the optical turbulence profile than existing large telescopes. These telescopes will be sensitive to variations in the altitude

Further author information: (Send correspondence to J.O.)

J.O.: E-mail: james.osborn@durham.ac.uk

of optical turbulence. As a basic calculation we can say that the native resolution of the wide-field AO system will be,

$$\delta h = \frac{h_{\max}}{n_{\text{sub}}}, \quad (1)$$

where h_{\max} is the maximum altitude of the turbulence, usually taken to be the maximum altitude of the tropopause (latitude dependent but taken here as ~ 25 km) and n_{sub} is the number of AO subapertures across the telescope pupil. As an example, although still under active development, the current baseline for the European-ELT Multi-Object Spectrograph, MOSAIC,² is for $n_{\text{sub}}=74$, resulting in a native resolution of ~ 350 m. However, it is likely that the AO system will actually be sensitive to changes of altitude smaller than this. This is because small changes in turbulence altitude can subtly change the correlation matrix between the different wavefront sensors and impact the performance of the instrument. More detailed analyses show that the required altitude resolution of the turbulence profile is 100 to 500 m.³⁻⁷

The three most prevalent optical profiling techniques in operation today are MASS (Multi Aperture Scintillation System⁸), SCIDAR (SCIntillation Detection And Ranging⁹) and SLODAR (SLOPe Detection And Ranging¹⁰). MASS is not intended as a high vertical-resolution technique. It has a limited logarithmic vertical resolution and the high altitude response is very broad.⁸ Both SLODAR and SCIDAR are triangulation techniques in which the atmospheric turbulence profile is recovered from either the correlation of wavefront slopes in the case of SLODAR, or scintillation intensity patterns in the case of SCIDAR, for two target stars with a known angular separation. Generalised-SCIDAR¹¹ is a development of the SCIDAR technique where the detectors are conjugate below the ground level in order to make the instrument sensitive to turbulence at the ground.

The theoretical resolution for Generalised-SCIDAR varies with the Fresnel zone size for a given altitude of the turbulent layer and is given by,¹²

$$\delta h(z) = 0.78 \frac{\sqrt{\lambda z}}{\theta}, \quad (2)$$

where λ is the wavelength, θ is the separation of the double star and z is the propagation distance to the layer. z depends on both the airmass of the observation ($\sec(\theta_z)$, where θ_z , is the zenith angle) and the conjugate altitude of the detector plane, h_{conj} , and is given by, $z = |h + h_{\text{conj}} \sec(\theta_z)|$. h is the altitude of the turbulent layer. For larger propagation distances the spatial scale of the intensity speckle patterns is larger, reducing the altitude resolution. Therefore the native altitude resolution of Generalised-SCIDAR is altitude dependent with a significantly reduced resolution for high-altitude turbulence. As with SLODAR, in order to achieve 200 m altitude resolution to 20 km with Generalised-SCIDAR an 8 m telescope is required.⁶

Egner & Masciadri¹³ proposed a way to increase the altitude resolution of Generalised-SCIDAR based on simultaneous turbulence velocity profiles. To implement this High-Vertical Resolution (HVR) mode the profiler needs to be able to measure the vertical profile of the turbulence velocity in addition to the strength. The approach taken is to track the position of the covariance peaks in the spatio-temporal cross-covariance function. Using the frame rate and pixel size the turbulence velocity can be estimated. Differential velocity vectors within a vertical resolution element signify different turbulent layers and can provide a vertical resolution higher than the native resolution of the instrument. Although turbulence velocity profiling has been demonstrated with SLODAR (for example¹⁴⁻¹⁶) and Generalised-SCIDAR (for example,^{17,18}) an automated approach is difficult.

Stereo-SCIDAR^{19,20} is a Generalised-SCIDAR instrument which is designed to measure the vertical profile of optical turbulence strength and velocity in the full atmosphere. In contrast to most SCIDAR instruments, Stereo-SCIDAR uses two cameras, one to image the defocussed pupil of each of the two target stars. By doing this the intensity of the images can be normalised independently, and hence Stereo-SCIDAR has increased sensitivity to weaker layers and can operate with a larger difference in brightness of the target stars. In addition, the spatial cross-covariance function has only one covariance peak per turbulent layer. This lends itself to automated turbulence velocity identification of the full atmosphere.²¹

Stereo-SCIDAR can use the automated velocity profiles with the HVR technique of Egner & Masciadri¹³ to measure the optical turbulence with ELT-scale altitude resolution. In addition, the turbulence velocity identification can be used to confirm the existence of weak turbulent layers close to the noise floor of the instrument. If a covariance peak is seen to move in the spatio-temporal covariance function then we can confirm

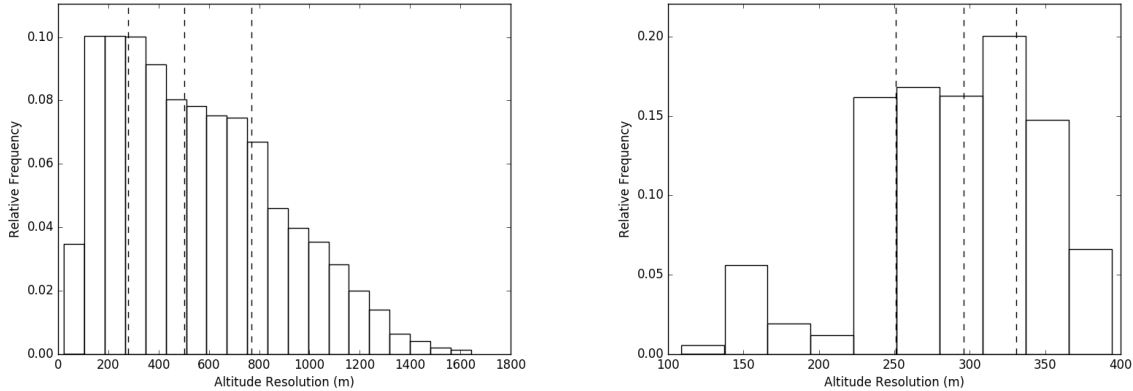


Figure 1. Histogram of altitude resolution with Stereo-SCIDAR on the INT, La Palma. The median altitude resolution measured was 520 m (left). In high-vertical resolution mode, the median altitude resolution was 300 m (right)

that it is real and not simply noise, which would behave differently. These layers could easily be ignored in the data analysis but for applications where high sensitivity is required, they could be important. However, before this data can be used in performance simulations for future ELT instrumentation the automated turbulence velocity identification must be validated.

At the time of writing only one complete night of commissioning data has been recorded with Stereo-SCIDAR at cerro Paranal. However, Stereo-SCIDAR will be operated at cerro Paranal for several nights every month for at least the next year. This data will be of critical importance for studies for the next generation of ELTs.²² For this study we make use of previous stereo-SCIDAR data on the Isaac Newton Telescope, La Palma. As the two system are very similar we assume that the altitude resolution, turbulence velocity and turbulence strength identification performance will be comparable.

2. STEREO-SCIDAR

Stereo-SCIDAR is an instrument designed to measure the vertical profile of the optical turbulence with high-altitude resolution and high-sensitivity. Stereo-SCIDAR is based on a generalised-SCIDAR technique.

Contrasting most SCIDAR instruments, Stereo-SCIDAR uses two cameras, one to image the defocused pupil of each of the two target stars. A reflective wedge near to the focal plane is used to separate the light from the two target stars. By doing this Stereo-SCIDAR has increased sensitivity to weaker layers, can operate with a larger difference in brightness of the target stars and has only one covariance peak per turbulent layer. The latter lends itself to automated turbulence velocity identification of the full atmosphere.^{21,23}

In High-Vertical Resolution (HVR) mode,¹³ we can use the detected turbulence vectors in order to define the altitude of a turbulent layer to a much higher precision than is usually possible.²³ In this way Stereo-SCIDAR can be used to measure the optical turbulence with the same altitude resolution that will be expected from the AO telemetry on an ELT.²⁴

2.1 Altitude resolution

The altitude resolution of Stereo-SCIDAR, as with all SCIDAR instruments, is altitude dependent. Figure 1 (left) shows the distribution of measured altitude resolutions from the Stereo-SCIDAR data. The shape of the distribution can be explained by the fact that there is more data at lower altitudes as the maximum altitude is dependent on both the angular separation of the target stars and the airmass of the telescope pointing. The median altitude resolution is ~ 500 m. This data has an altitude resolution which is acceptable for most applications (e.g. instrument modelling for 8 m class telescopes), however, for the most demanding cases, wide-field AO modelling for ELT scale instrumentation, this native vertical fidelity is not satisfactory.

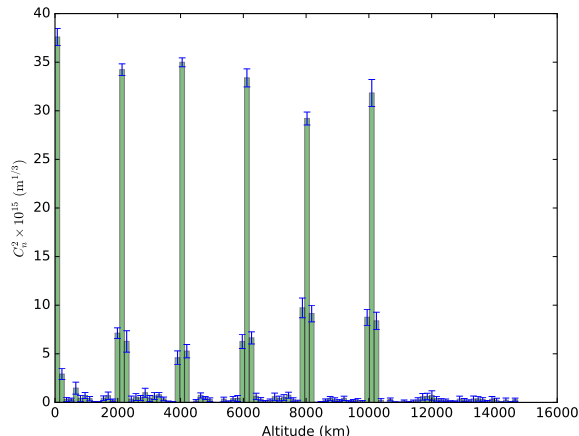


Figure 2. Simulated profile from a Monte-Carlo simulation linked into the Stereo-SCIDAR real-time data analysis pipeline. The input profile was for a fictional atmosphere consisting of six layers of equal strength at 0, 2, 4, 6, 8 and 10 km. The input turbulence strength was $3.54 \times 10^{-13} \text{ m}^{1/3}$ ($r_0 = 0.15 \text{ cm}$). The integrated output turbulence strength is $3.09 \times 10^{-13} \text{ m}^{1/3}$ ($r_0 = 0.16 \text{ m}$).

In HVR mode the altitude resolution of Stereo-SCIDAR is significantly increased (figure 1, right). In HVR mode there is less variation in the vertical altitude resolution. In this case we identify the altitude of a layer to the nearest pixel. This yields an altitude resolution that is independent of altitude and has a median value of 300 m. It should be noted that a sub-pixel resolution is possible with this method but that is not currently implemented to aid robustness.

As previously discussed, the large number of subapertures across the AO system pupil means that the next generation of 30 to 40 m class Extremely Large Telescopes (ELTs) will be significantly more sensitive to variations in the optical turbulence profile than existing 8 m class systems. These telescopes will be sensitive to variations in turbulence altitude of the order of 100 to 500 m.

This altitude resolution from stereo-SCIDAR is now high enough to be valuable for even wide-field modelling of future ELT instrumentation.

3. VALIDATION

3.1 Simulated atmospheric turbulence profile

The real-time data analysis pipeline has been tested by using a Monte-Carlo simulation as an input. This scintillation simulation has been developed by the authors and has been intensively tested for this purpose (see for example²⁵). Figure 2 shows the output profile for a fictional turbulence profile, consisting of six equal strength layers of $C_n^2 dh = 5.3 \times 10^{-14} \text{ m}^{-2/3}$ each. The total integrated turbulence strength is $C_n^2 dh = 3.2 \times 10^{-13} \text{ m}^{-2/3}$ ($r_0 = 0.16 \text{ m}$). It can be seen that the peak turbulence strength of each layer is lower than the expected $5.3 \times 10^{-14} \text{ m}^{-2/3}$. This is because the altitude resolution of the SCIDAR instrument is larger than the size of a pixel and so the signal is spread over several peaks in the resultant profile.

3.2 Automated wind velocity identification

To validate the wind velocity identification, we compare wind and turbulence velocity profiles from three sources:

- physical tracking measurements of balloon borne radiosondes via a Global Positioning System and radio-theodolite.²⁶
- computer model, Global Forecast System (GFS) meteorological forecasts provided by the National Oceanic and Atmospheric Administration.²⁷

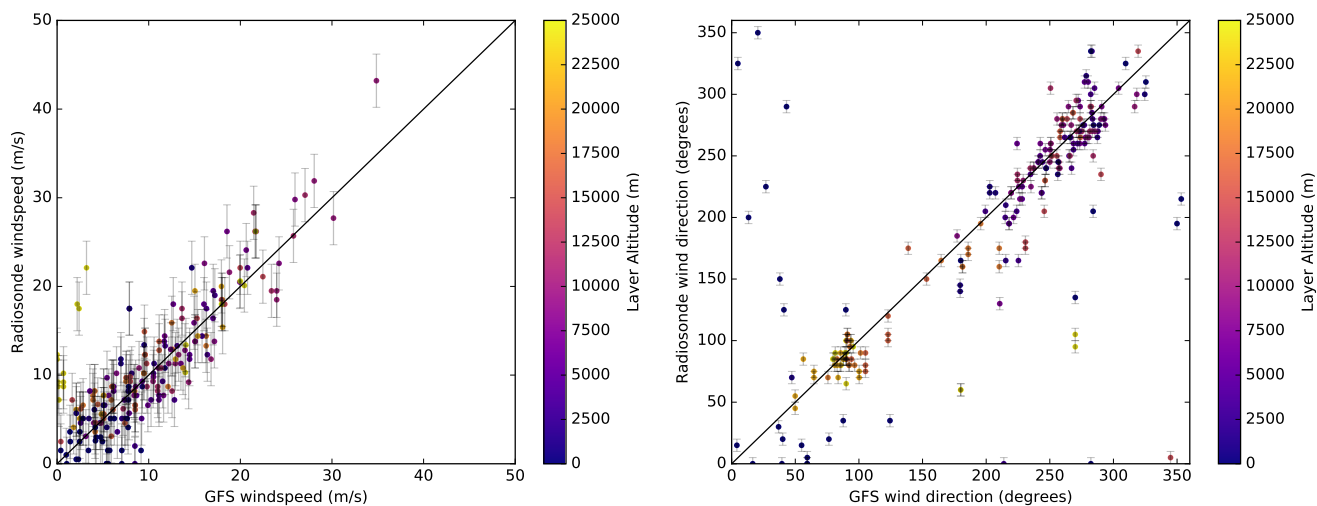


Figure 3. Comparison of wind speed (left) and wind direction (right) from radiosonde and GFS. The correlation coefficients are 0.86 and 0.93 respectively

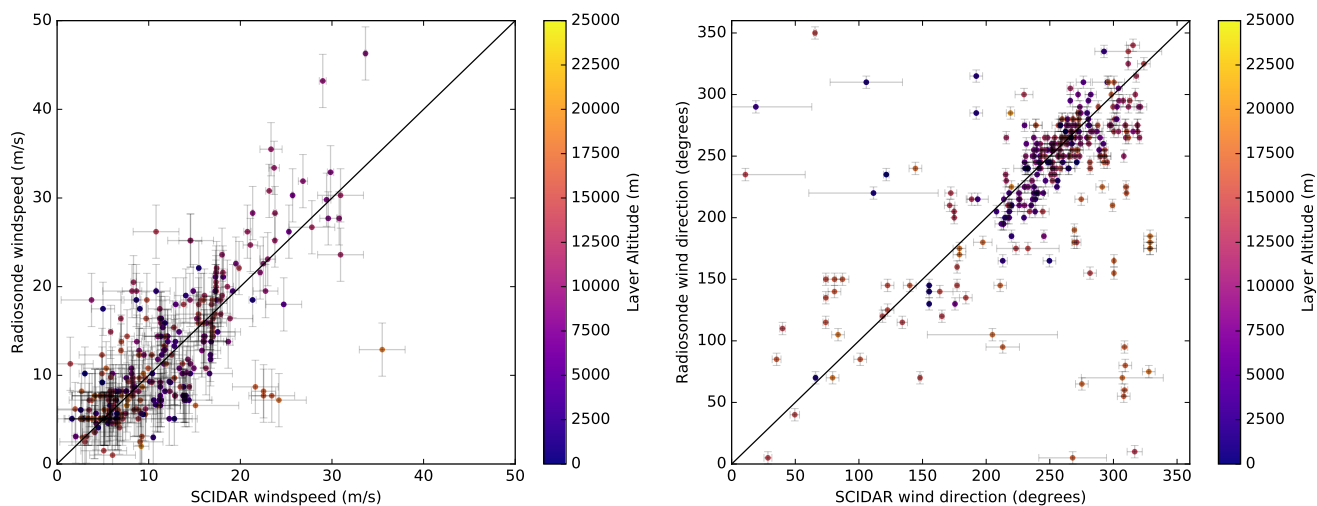


Figure 4. Comparison of wind speed (left) and wind direction (right) from radiosonde and Stereo-SCIDAR. The correlation coefficients are 0.75 and 0.84 respectively

- optical remote sensing, Stereo-SCIDAR automated wind velocity detection algorithm.

These data sources were chosen for our comparison as both the measured radiosonde and modelled GFS wind velocities have been shown to provide precise estimates (for example, [18, 28–30](#)).

With this cross-validation we show that the turbulence and the wind velocity are highly correlated, simultaneously showing that the Stereo-SCIDAR turbulence velocity is precise and that the numerical models of the wind velocity can be used as an estimator for the turbulence velocity.

4. PARANAL PROFILE

Figure 6 shows the first stereo-SCIDAR turbulence strength and velocity profile from cerro Paranal. The profile of this one night shows variable conditions in terms of turbulence altitude and strength. The stereo-SCIDAR will operate at cerro Paranal for several nights per month for at least the next year.

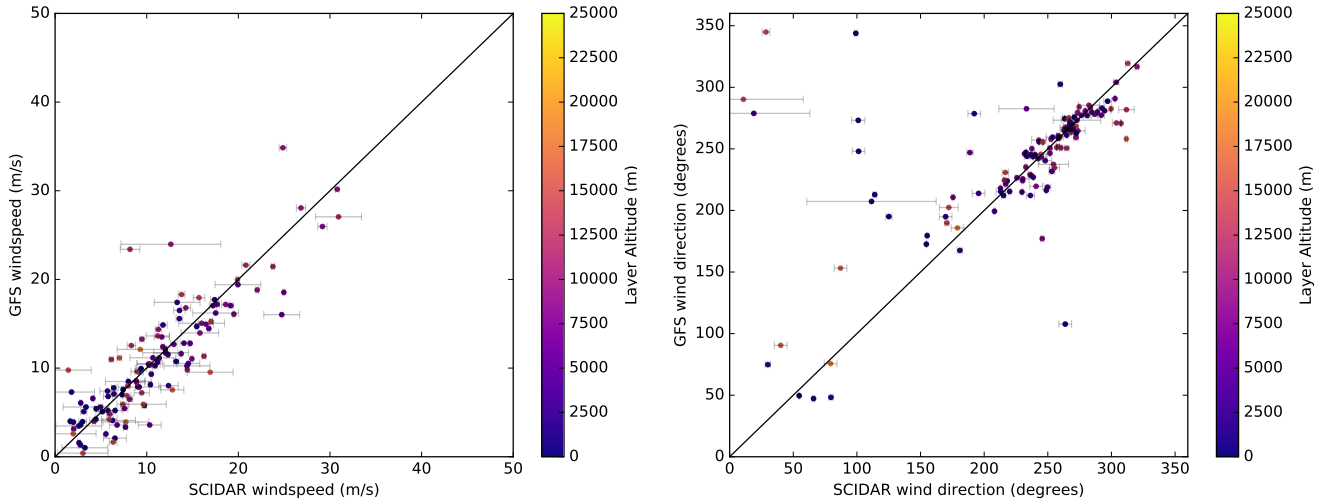


Figure 5. Comparison of wind speed (left) and wind direction (right) from GFS and Stereo-SCIDAR. The correlation coefficients are 0.85 and 0.91 respectively

5. CONCLUSIONS

Stereo-SCIDAR, a high-altitude resolution atmospheric turbulence profiler has been commissioned on one of the 1.8 m Auxiliary Telescopes at Cerro Paranal. Cerro Paranal is the site of the Very Large Telescope and only 50 km from the future European-Extremely Large Telescope. The data from Stereo-SCIDAR is therefore critical for design studies of E-ELT instrumentation as well as performance monitoring and optimisation of existing VLT and future E-ELT operations.

We use data taken with stereo-SCIDAR at La Palma to demonstrate that the stereo-SCIDAR is capable of 300 m altitude resolution, and that the automated turbulence velocity identification correlates well with both in-situ radiosonde measurements and numerical atmospheric models.

ACKNOWLEDGMENTS

We are grateful to the Science and Technology Facilities Committee (STFC) for financial support (grant reference ST/J001236/1). FP7/2013-2016: The research leading to these results has received funding from the European Community’s Seventh Framework Programme (FP7/2013-2016) under grant agreement number 312430 (OPTICON). The Isaac Newton Telescope is operated on the island of La Palma by the Isaac Newton Group in the Spanish Observatorio del Roque de los Muchachos of the Instituto de Astrofísica de Canarias. We are also grateful to the NOAA Earth System Research Laboratory for making the radiosonde and Global Forecast System (GFS) meteorological forecast data available on the web. The Stereo-SCIDAR data used in this project is available upon request from the authors.

REFERENCES

- [1] Osborn, J., Föhring, . D., Dhillon, V. S., and Wilson, R. W., “Atmospheric scintillation in astronomical photometry,” *MNRAS* **452**, 1707–1716 (2015).
- [2] Evans, C. J., Puech, M., Barbuy, B., Bonifacio, P., Cuby, J. G., Guenther, E., Hammer, F., Jagourel, P., Kaper, L., Morris, S. L., Afonso, J., Amram, P., Aussel, H., Basden, A., Bastian, N., Battaglia, G., Biller, B., Bouché, N., Caffau, E., Charlot, S., Clenet, Y., Combes, F., Conselice, C., Contini, T., Dalton, G., Davies, B., Disseau, K., Dunlop, J., Fiore, F., Flores, H., Fusco, T., Gadotti, D., Gallazzi, A., Giallongo, E., Gonçalves, T., Gratadour, D., Hill, V., Huertas-Company, M., Ibata, R., Larsen, S., Fèvre, O. L., Lemasle, B., Maraston, C., Mei, S., Mellier, Y., Östlin, G., Paumard, T., Pello, R., Pentericci, L., Petitjean, P., Roth, M., Rouan, D., Schaerer, D., Telles, E., Trager, S., Welikala, N., Zibetti, S., and Ziegler, B., “Science Case

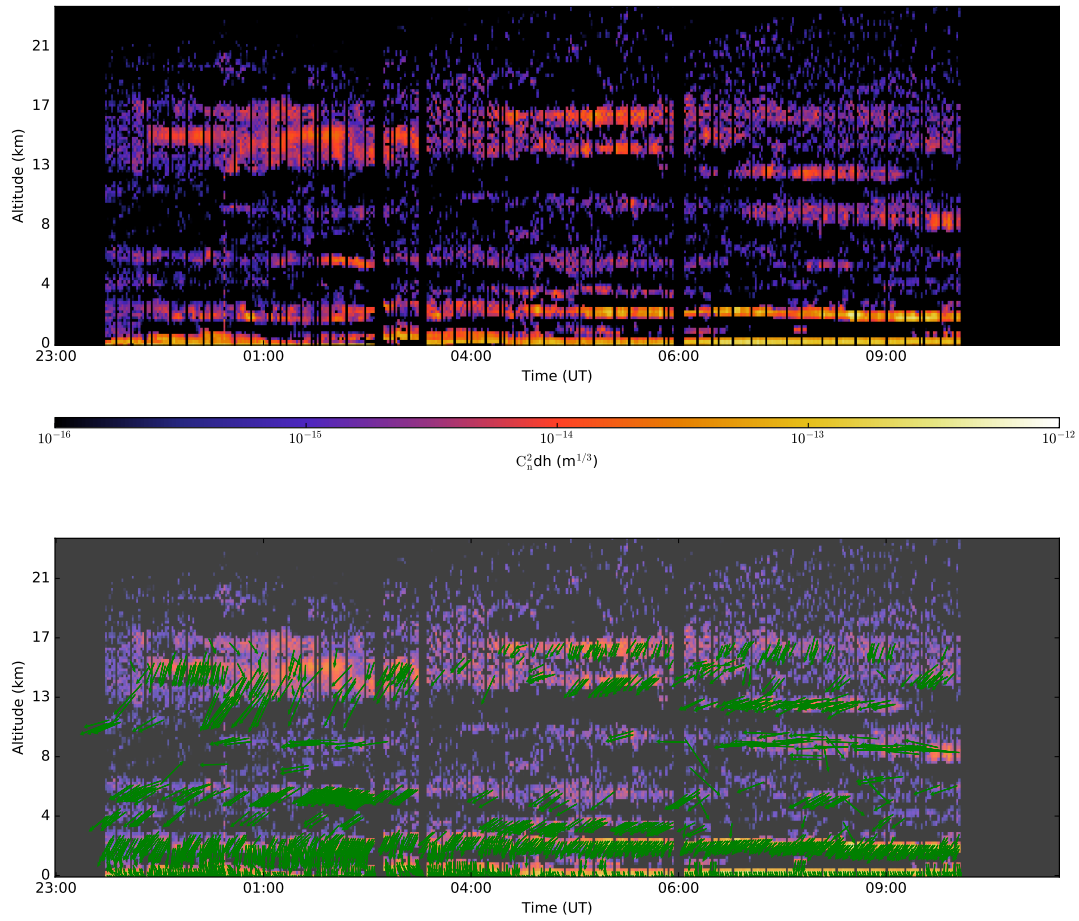


Figure 6. Stereo-SCIDAR profiles from 29th April 2016 at Cerro Paranal. The top plot is the optical turbulence profile through the night (the colourbar indicates the strength of the turbulence) and the lower plot has the wind vectors overlaid. Only a subset of wind vectors are shown for clarity. The figure shows the high variability of the turbulence throughout the night, both in terms of strength and altitude.

and Requirements for the MOSAIC Concept for a Multi-Object Spectrograph for the European Extremely Large Telescope,” 17 (7 2014).

- [3] Neichel, B., Fusco, T., and Conan, J.-M., “Tomographic reconstruction for wide-field adaptive optics systems: Fourier domain analysis and fundamental limitations,” *Journal of the Optical Society of America A* **26**, 219 (12 2008).
- [4] Basden, A., Myers, R., and Butterley, T., “Considerations for EAGLE from Monte Carlo adaptive optics simulation,” *Appl. Opt.* **49**(31), G1–G8 (2010).
- [5] Vidal, F., Gendron, E., and Rousset, G., “Tomography approach for multi-object adaptive optics,” *J. Opt. Soc. Am. A.* **27**(11), 253–264 (2010).
- [6] Masciadri, E., Rousset, G., Fusco, T., Bonifacio, P., Fuensalida, J. J., Robert, C., Sarazin, M., Wilson, R. W., and Ziad, A., “A roadmap for a new era turbulence studies program applied to the ground-based astronomy supported by AO,” in [AO4ELT3], (2013).
- [7] Gendron, E., Morel, C., Osborn, J., Martin, O., Gratadour, D., Vidal, F., Le Louarn, M., and Rousset, G., “Robustness of tomographic reconstructors versus real atmospheric profiles in the ELT perspective,” in [*SPIE Astronomical Telescopes + Instrumentation*], Marchetti, E., Close, L. M., and Véran, J.-P., eds., 91484N, International Society for Optics and Photonics (8 2014).
- [8] Tokovinin, A. and Kornilov, V., “Accurate seeing measurements with MASS and DIMM,” *MNRAS* **381**, 1179–1189 (2007).
- [9] Vernin, J. and Roddier, F., “Experimental determination of two-dimensional spatiotemporal power spectra of stellar light scintillation Evidence for a multilayer structure of the air turbulence in the upper troposphere,” *Journal of the Optical Society of America* **63**(3), 270 (1973).
- [10] Wilson, R. W., “SLODAR: Measuring optical turbulence altitude with a Shack-Hartmann wavefront sensor,” *Monthly Notices of the Royal Astronomical Society* **337**(1), 103–108 (2002).
- [11] Fuchs, A., Tallon, M., and Vernin, J., “Folding-up of the vertical atmospheric turbulence profile using an optical technique of movable observing plane,” in [*SPIE*], 682–692 (1994).
- [12] Prieur, J. L., Daigne, G., and Avila, R., “SCIDAR measurements at Pic du Midi,” *A&A* **371**, 366–377 (2001).
- [13] Egner, S. and Masciadri, E., “A G-SCIDAR for Ground-Layer Turbulence Measurements at High Vertical Resolution,” *Publications of the Astronomical Society of the Pacific* **119**(862), 1441–1448 (2007).
- [14] Cortes, A., Neichel, B., Guesalaga, A., Osborn, J., Rigaut, F., and Guzman, D., “Atmospheric turbulence profiling using multiple laser star wavefront sensors,” *Monthly Notices of the Royal Astronomical Society* **427**(3), 2089–2099 (2012).
- [15] Guesalaga, A., Neichel, B., Cortes, A., Bechet, C., and Guzman, D., “Using the $\$C_n^2\$$ and wind profiler method with wide-field laser-guide-stars adaptive optics to quantify the frozen-flow decay,” *Monthly Notices of the Royal Astronomical Society* **440**, 1925–1933 (4 2014).
- [16] Gilles, L. and Ellerbroek, B., “Wind profiling via slope detection and ranging: algorithm formulation and performance analysis for laser guide star tomography on extremely large telescopes,” *Proceedings of the Third AO4ELT Conference. Firenze* (2013).
- [17] Prieur, J. L., Avila, R., Daigne, G., and Vernin, J., “Automatic Determination of Wind Profiles with Generalized SCIDAR,” *PASP* **116**, 778–789 (2004).
- [18] García-Lorenzo, B. and Fuensalida, J. J., “Processing of turbulence-layer wind speed with Generalized SCIDAR through wavelet analysis,” *MNRAS* **372**, 1483–1495 (2006).
- [19] Shepherd, H., Osborn, J., Wilson, R. W., Butterley, T., Avila, R., Dhillon, V., and Morris, T. J., “Stereo-SCIDAR: High altitude-resolution optical turbulence profiling using a modified SCIDAR instrument,” *MNRAS* **437**(4), 3568–3577 (2013).
- [20] Osborn, J., Wilson, R. W., Shepherd, H., Butterley, T., Dhillon, V. S., and Avila, R., “Stereo SCIDAR: Profiling atmospheric optical turbulence with improved altitude resolution,” in [*Proceedings of the Third AO4ELT Conference*], Esposito, S. and Fini, L., eds., INAF - Osservatorio Astrofisico di Arcetri, Firenze (2013).
- [21] Osborn, J., Butterley, T., Föhring, D., and Wilson, R., “Characterising atmospheric optical turbulence using stereo-SCIDAR,” *Journal of Physics: Conference Series* **595**(1) (2015).

- [22] Osborn, J., Butterley, T., Perera, S., Fohring, D., and Wilson, R. W., “Observations of the dynamic turbulence above La Palma using Stereo-SCIDAR,” in *[AO4ELT4]*, (2015).
- [23] Osborn, J., Butterley, T., Townson, M. J., Reeves, A. P., Morris, T. J., and Wilson, R. W., “Wind and turbulence velocity profiling for high sensitivity and vertical-resolution atmospheric characterisation with Stereo-SCIDAR,” *MNRAS in prep* (2016).
- [24] Osborn, J., Butterley, T., and Wilson, R. W., “Stereo-SCIDAR optical turbulence characterisation from La Palma,” *MNRAS* (2016).
- [25] Osborn, J., Wilson, R. W., Dhillon, V., Avila, R., and Love, G. D., “Conjugate Plane Photometry: Reducing Scintillation for Ground-Based Fast Photometry,” *MNRAS* **411**(2), 1223–1230 (2011).
- [26] NOAA, [*Federal Meteorological Handbook No. 3*] (1997).
- [27] NOAA/NCEP, “Global Forecast System (GFS) Atmospheric Model,” (2015).
- [28] Sarazin, M., Cuevas, O., and Navarrete, J., “VERIFICATION OF THE COHERENCE TIME PRODUCED BY THE MASS-DIMM TURBULENCE PROFILER IN CHILE,” *Revista Mexicana de Astronomía y Astrofísica* **41**, 42–45 (2011).
- [29] Vernin, J., Barletti, R., Ceppatelli, G., Paternò, L., Righini, A., and Speroni, N., “Optical remote sensing of atmospheric turbulence: a comparison with simultaneous thermal measurements.,” *Applied optics* **18**(2), 243–7 (1979).
- [30] Avila, R., Masciadri, E., Vernin, J., and Sánchez, L. J., “Generalized SCIDAR Measurements at San Pedro M{á}rtir. I. Turbulence Profile Statistics,” *PASP* **116**, 682–692 (2004).